Journal of Zhejiang University-SCIENCE A (Applied Physics & Engineering)

Analysis of piston-pin lubrication considering the effects of structure deformation and cavitation*

Lin BA †1, Zhen-peng HE†‡2, Yue-hui LIU3, Gui-chang ZHANG2

(1School of Materials Science and Engineering, Tianjin University, Tianjin 300072, China)

(2Civil Aviation University of China , Aviation Institute of Automation, Tianjin 300300, China)

(3State Key Laboratory of Engines, Tianjin University, Tianjin 300072, China)

†E-mail: yeminghuangziji@163.com; hezhenpeng@tju.edu.cn

Cite this as: Lin Ba, Zhen-peng He, Yue-hui Liu, Gui-chang Zhang, 2015. Analysis of piston-pin lubrication considering the effects of structure deformation and cavitation. *Journal of Zhejiang University-SCIENCE A (Applied Physics & Engineering)*, 16(6):443-463. [doi:10.1631/jzus.A1400105]

Theory

$$\boldsymbol{M}\ddot{\boldsymbol{u}}+\boldsymbol{C}\dot{\boldsymbol{u}}+\boldsymbol{K}\boldsymbol{u}=\boldsymbol{F}$$

$$\begin{bmatrix}\boldsymbol{M}_{\mathrm{ii}} & \boldsymbol{M}_{\mathrm{ir}}\\ \boldsymbol{M}_{\mathrm{ri}} & \boldsymbol{M}_{\mathrm{rr}}\end{bmatrix}\begin{Bmatrix}\ddot{\boldsymbol{u}}_{\mathrm{i}}\\ \ddot{\boldsymbol{u}}_{\mathrm{r}}\end{Bmatrix}+\begin{bmatrix}\boldsymbol{C}_{\mathrm{ii}} & \boldsymbol{C}_{\mathrm{ir}}\\ \boldsymbol{C}_{\mathrm{ri}} & \boldsymbol{C}_{\mathrm{rr}}\end{bmatrix}\begin{Bmatrix}\dot{\boldsymbol{u}}_{\mathrm{i}}\\ \dot{\boldsymbol{u}}_{\mathrm{r}}\end{Bmatrix}+\begin{bmatrix}\boldsymbol{K}_{\mathrm{ii}} & \boldsymbol{K}_{\mathrm{ir}}\\ \boldsymbol{K}_{\mathrm{ri}} & \boldsymbol{K}_{\mathrm{rr}}\end{bmatrix}\begin{Bmatrix}\boldsymbol{u}_{\mathrm{i}}\\ \boldsymbol{u}_{\mathrm{r}}\end{Bmatrix}=\begin{bmatrix}\boldsymbol{F}_{\mathrm{i}}\\ \boldsymbol{F}_{\mathrm{r}}\end{bmatrix}$$

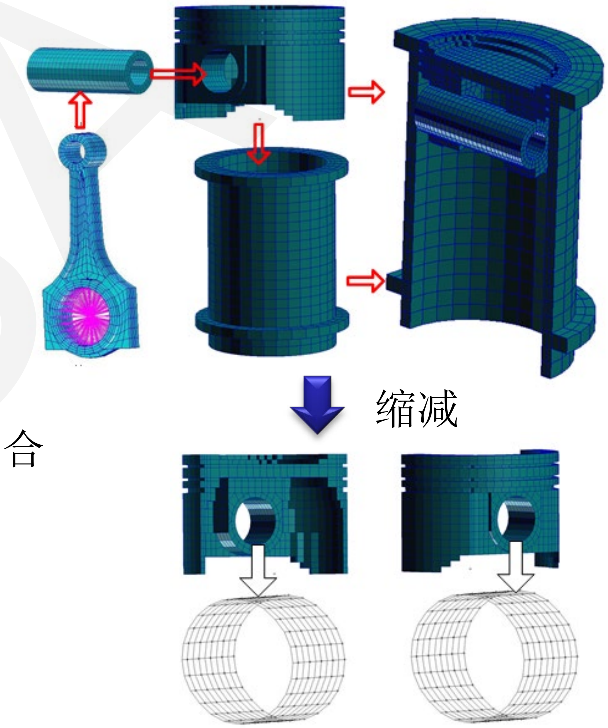

缩减

耦合

$$\frac{\partial}{\partial x}\left(\frac{h^3}{\eta}\frac{\partial p}{\partial x}\right)+\frac{\partial}{\partial z}\left(\frac{h^3}{\eta}\frac{\partial p}{\partial z}\right)=6(u_1+u_2)\frac{\partial h}{\partial x}+12\frac{\partial(h)}{\partial t}$$

$$P_{\mathrm{asp}}=\frac{16\sqrt{2}\pi}{15}(\sigma\beta'\eta')^2\sqrt{\frac{\sigma}{\beta}}E'F_{5/2}(H)$$

有限元与有限差分插值

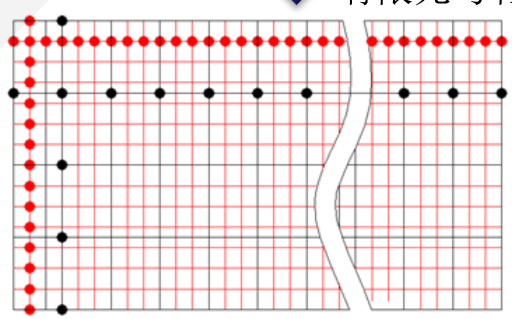

Cavitation

Lubrication

Analysis

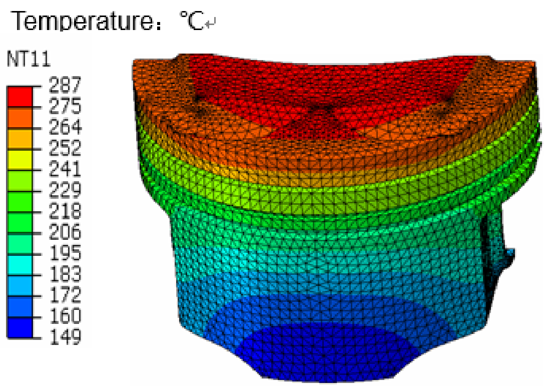

Thermal analysis

Thermal analysis verification

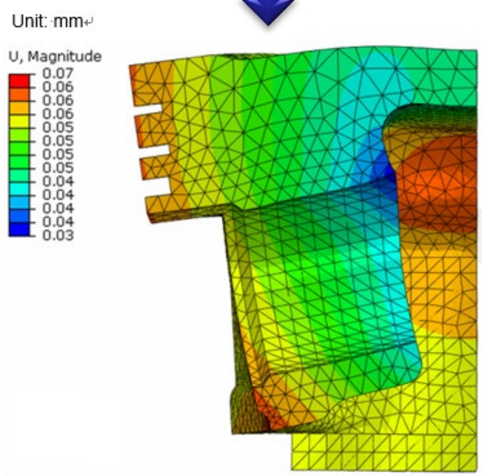

Thermal deformation analysis

Basic lubrication performance

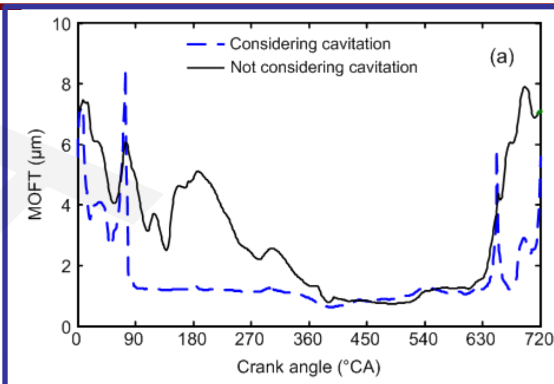

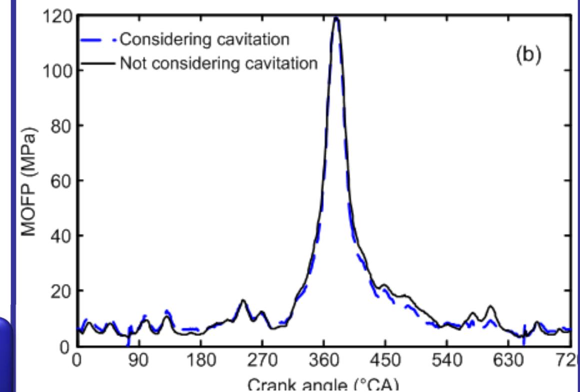

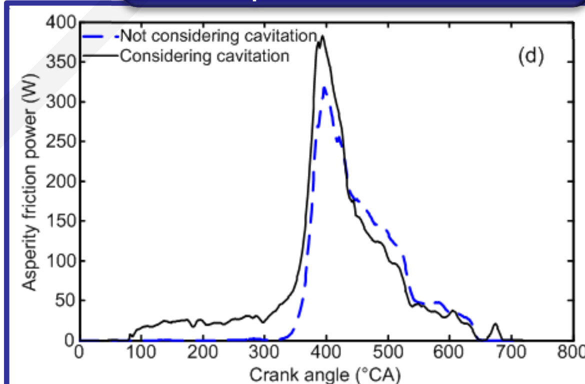

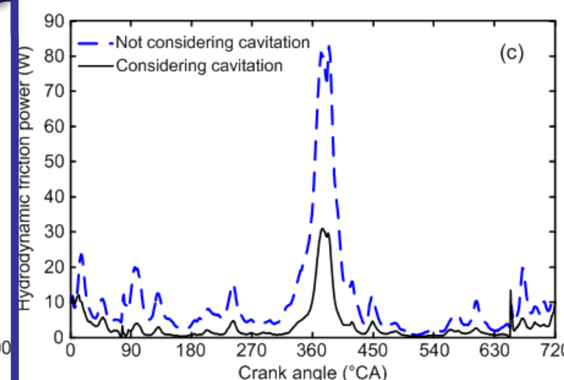

The effect of parameters on piston pin lubrication performances

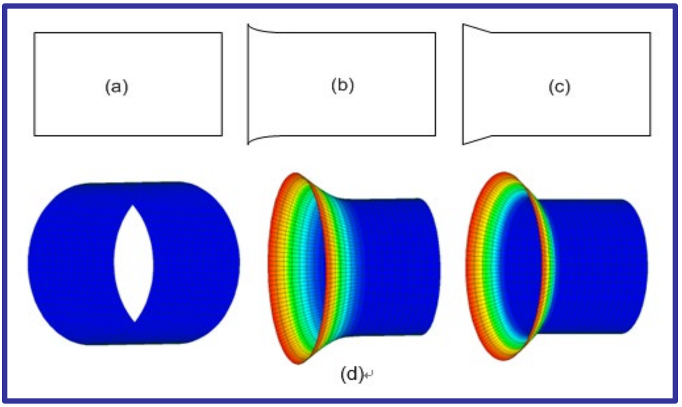

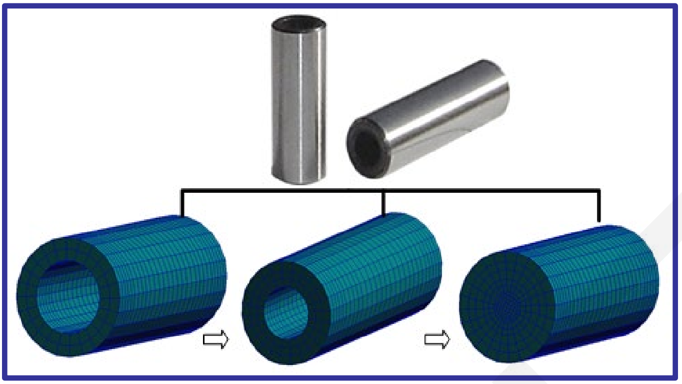

Thermal deformation

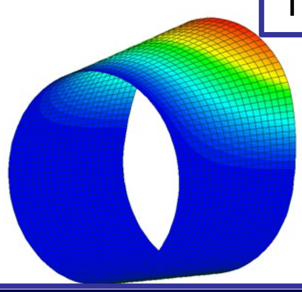

Performances under different profiles

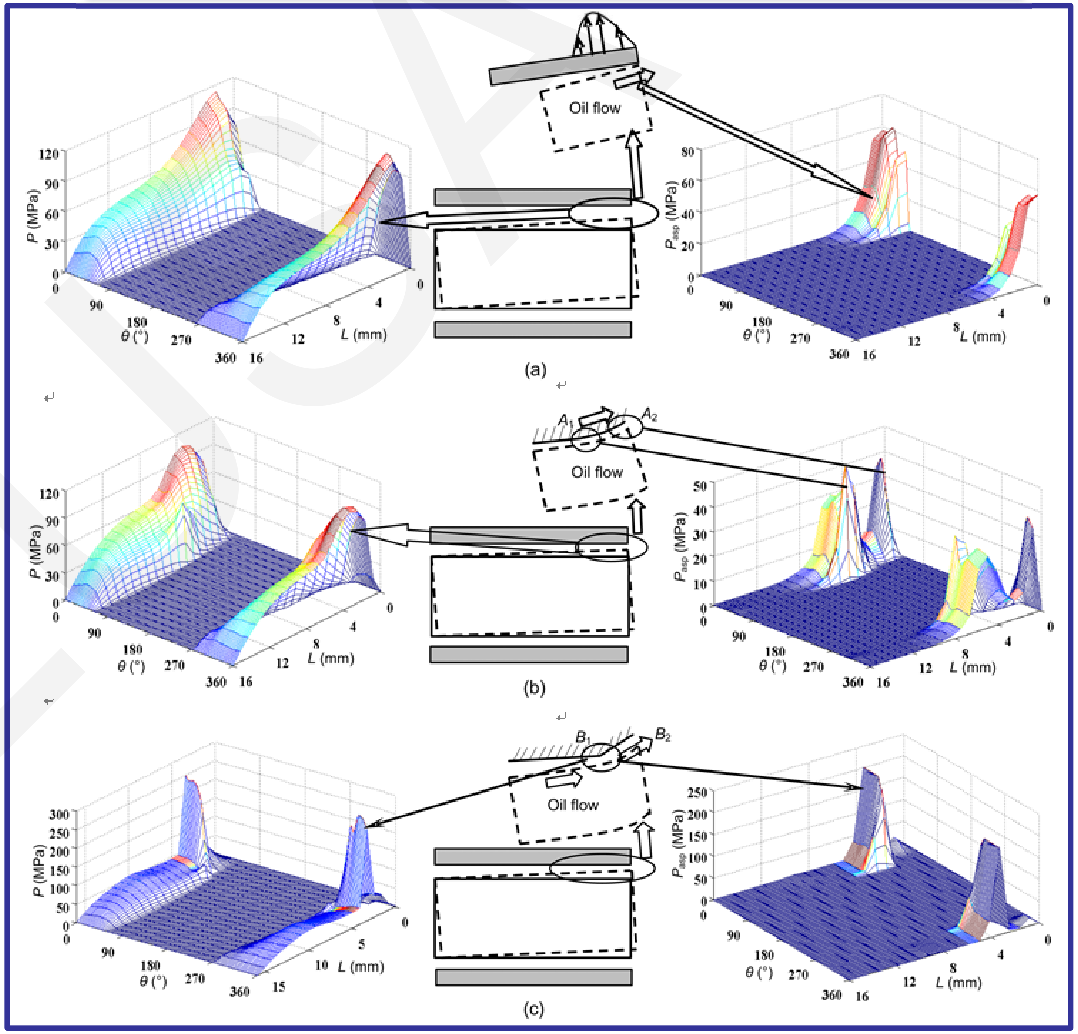

The effect of parameters on piston pin lubrication performances

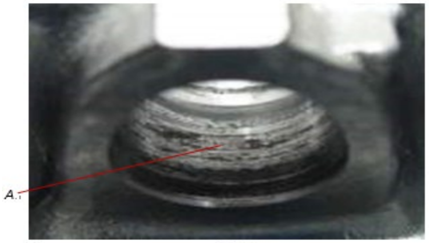

(a)

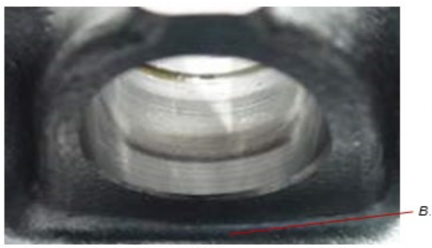

(b)

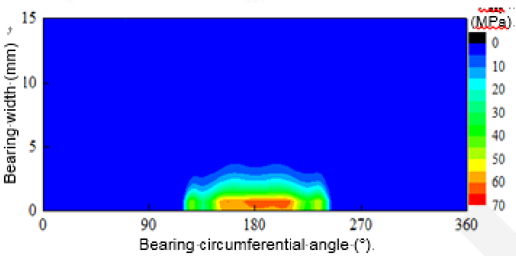

(c)

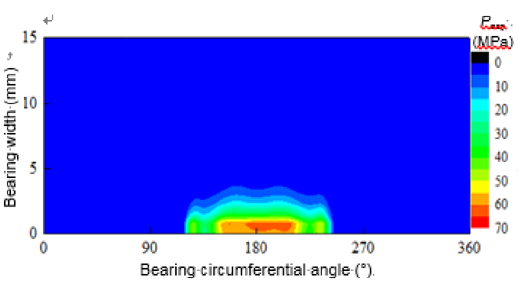

(d)

Asperity contact verification

Performances under different hole diameters

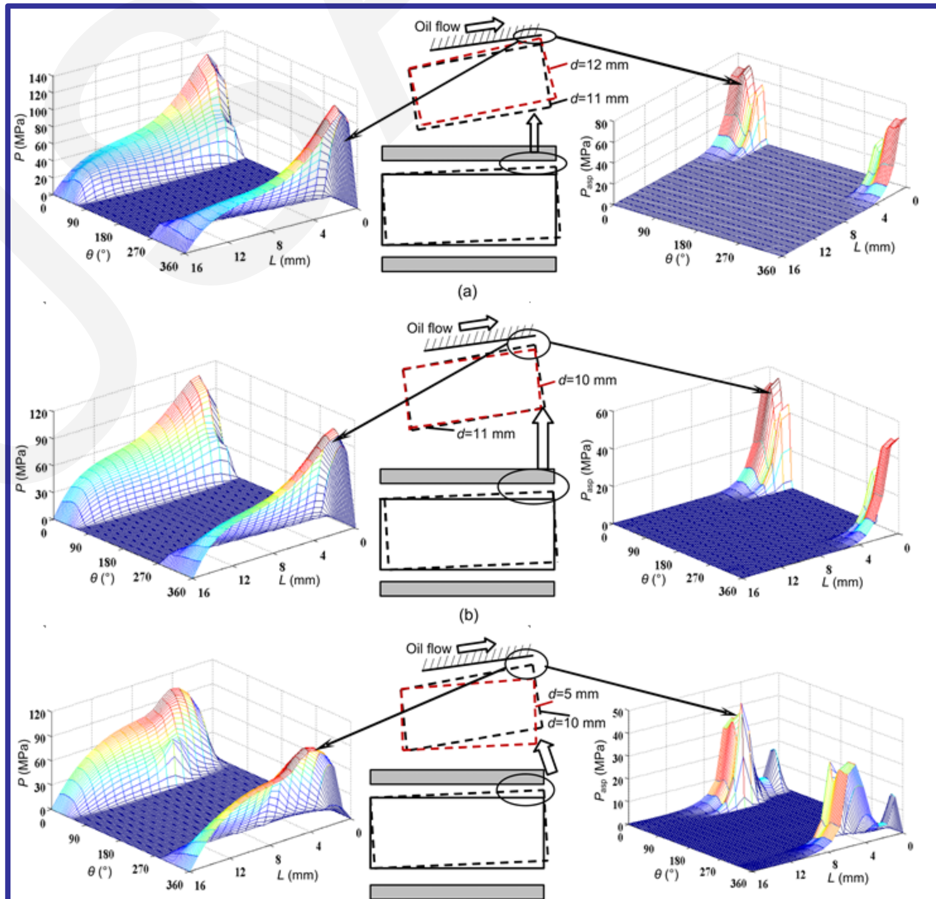

Conclusions

- A multi-body dynamic model for the piston system based on component mode synthesis method is established. The elastic deformation and cavitation are considered in the model. To solve the mismatch of coarse finite element mesh and fine finite difference mesh, a 2D interpolation method is introduced to the model, and then a coarse FEM mesh density can be used for bearing structure to reduce the amount of computation. Fine finite difference mesh helps to solve the problem of sharp gradients resulting from the eccentric position of the piston pin.
- The lubrication analysis of the piston pin combined with the deformation of the pin is implemented. When the peak cylinder pressure acts on the top surface of the piston crown, and the connecting rod supports the pin, this causes the pin to be misaligned. This is why the asperity contact occurs at the inside of the pin bore.
- Comparing all the pressure results calculated with the traditional model, the result shows that the trends of the MOFT and MOFP are nearly the same. However, the MOFT calculated with the traditional model is obviously different from that using the cavitation model. They appear at different crank angles for the two different models, i.e., 483 ° CA and 384 ° CA, respectively. The pressure distributions at some typical crank angles are compared. What causes the MOFP to be different is that some regions do not compact the load due to the oil film rupture. The pressure compacting region is consistent with the density due to the oil film compressibility.
- The oil film pressure and asperity contact pressure at peak cylinder pressure are compared for three different bin bore profiles: square profile, parabola profile, and flare profile. Parabolic profile can reduce the wear to some extent. However, flare profile intensifies the wear of some places, but reduces the regions. The reasons for these differences are explained. All the results can provide guidance for the design of the pin bore.